Pattern Formation Due to Spin-Wave Instabilities: Squares, Hexagons, and Quasiperiodic Patterns

Franz-Josef Elmer
Institut für Physik, Universität Basel, CH-4056 Basel, Switzerland
(Received 21 December 1992)

We study dissipative patterns caused by spin-wave instabilities in insulating ferromagnetic films which are driven by out-of-plane parallel pumping. Using a multiple-scale perturbation method, we derive amplitude equations for magnetostatic modes with wavelengths much larger than the film thickness, and study the stability of solutions with constant amplitudes. The main result is that the only stable patterns are squares, hexagons, and quasiperiodic patterns based on three standing waves. Quantitative results strongly support the suggestion that these patterns should be experimentally observable by means of Faraday rotation.

PACS numbers: 76.50.+g, 05.70.Ln

The emergence of wave patterns due to some instability mechanism in systems far from equilibrium is a general behavior in nature. These patterns and their formation have been intensively studied in fluid systems, especially in Rayleigh-Bénard convection, Taylor-Couette convection, electrohydrodynamic convection in liquid crystals [1], and Faraday instabilities of fluid-air interfaces [2].

More than forty years ago Bloembergen and Damon [3] found in high-power ferromagnetic resonance (FMR) of ferrites an anomaly (saturation of the main resonance) which was explained by Suhl [4] as an effect of a parametric resonance instability of certain spin waves. In the last decade this system has been investigated as an example of a nonlinear system showing deterministic chaos [5].

Most FMR experiments measure only global properties like the absorbed microwave power. Only a few experiments, all using inelastic Brillouin scattering as a tool, investigate the spatial properties of these patterns [6]. Up to now apparently no experiments have been performed which give either directly or indirectly a spatial image of these standing-wave patterns [7].

In this Letter we calculate the spatial patterns which emerge just above the instability threshold. We consider an infinitely extended insulating ferromagnetic film where the static field $\mathbf{H}$ and the driving field $\mathbf{h}$ are perpendicular to the film plane (i.e., out-of-plane parallel pumping), and derive amplitude equations from the basic Landau-Lifshitz equation:

$$\frac{1}{\gamma}\partial_t \mathbf{M} = -\mathbf{M}\times\mathbf{H}_{\text{eff}} - \frac{g}{M_0}\mathbf{M}\times(\mathbf{M}\times\mathbf{H}_{\text{eff}}), \qquad (1)$$

where $\mathbf{M}$ is the magnetization with $|\mathbf{M}(\mathbf{r},t)| = M_0$ the equilibrium magnetization, $\mathbf{H}_{\text{eff}}$ the effective magnetic field, γ the gyromagnetic ratio, and g a dimensionless damping parameter, which is directly given by the half-width of the resonance line divided by H. In the magnetostatic limit (i.e., electromagnetic wave propagation is negligible), the effective magnetic field of an isotropic parallel-pumped ferromagnet is

$$\mathbf{H}_{\text{eff}} = (H + h\cos\omega t)\mathbf{e}_z + D\nabla^2\mathbf{M} - \nabla\Phi_M, \qquad (2)$$

where $\mathbf{e}_z$ is the unit vector defined by the direction of the static field, ω is the frequency of the driving field, D the exchange stiffness constant, and Φ_M the magnetostatic potential which obeys the Poisson equation

$$\Delta\Phi_M = 4\pi\nabla\cdot\mathbf{M}. \qquad (3)$$

The boundary conditions are $|\nabla\Phi_M|(|z|\to\infty) = 0$ and $\partial_z\mathbf{M}(z=0) = \partial_z\mathbf{M}(z=d) = 0$, where d is the film thickness. We neglect any kind of surface pinning.

From bulk calculations it is well known that the most unstable modes are spin waves propagating in the plane perpendicular to the external fields [8]. At the threshold the uniform state bifurcates via a supercritical pitchfork bifurcation into a stationary state (stationary after a time average over the fast time scale given by $2\pi/\omega$).

Using a multiple-scale perturbation calculation one obtains a set of amplitude equations governing the dynamics near the threshold h_c:

$$\tau_0\frac{dA_j}{dt} = \epsilon A_j - c\left[|A_j|^2 + \sum_{l\neq j} a(\alpha_l-\alpha_j)|A_l|^2\right]A_j, \qquad (4)$$

where $\epsilon = (h-h_c)/h_c$, and A_j is the amplitude of a standing wave with the in-plane wave vector $\mathbf{k} = k_c(\mathbf{e}_x\cos\alpha_j + \mathbf{e}_y\sin\alpha_j)$. The coefficients τ_0, c, and a are real due to the fact that the bifurcation at the threshold is not a Hopf bifurcation. The coupling coefficient $a(\alpha)$ is a π-periodic function because of rotational symmetry, but $a(-\alpha)\neq a(\alpha)$ because the reflection symmetry is broken by the static field $\mathbf{H}$.

The magnetization $\mathbf{M}$ and the magnetostatic potential Φ_M are given in first order of the amplitudes A_j by

$$M_x + iM_y = M_0\sum_j e^{\pm i\alpha_j}[A_j(t)e^{ik_c(x\cos\alpha_j + y\sin\alpha_j)} + \text{c.c.}] \times m_\pm(z,t), \qquad (5)$$

$$\Phi_M = \frac{4\pi M_0}{k_c}\sum_j [iA_j(t)e^{ik_c(x\cos\alpha_j + y\sin\alpha_j)} + \text{c.c.}] \times\phi(z,t), \qquad (6)$$

where $m_\pm$ and ϕ are the time periodic solutions of

$$\partial_t m_\pm = \gamma(\pm i - g)[-DM_0\partial_z^2 m_\pm + 0(H - 4\pi M_0 + DM_0 k_c^2 + h_c\cos\omega t)m_\pm - 4\pi M_0\phi],$$
$$0 = \partial_z^2\phi - k_c^2\phi - k_c^2(m_+ + m_-)/2. \tag{7}$$

Note that $m_- = m_+^*$ because ϕ is real.

From the Floquet theorem it follows that the general solution of (7) is of the form $(m_\pm, \phi) = (\overline{m}_\pm, \overline{\phi})\exp(\lambda t)$, where $\overline{m}_\pm(z,t)$ and $\overline{\phi}(z,t)$ are $(2\pi/\omega)$-periodic functions in t. The stability of the uniform state $\mathbf{M} = M_0\mathbf{e}_z$ is determined by the "neutral curve" $h_{\rm nc}(k)$, which is defined by the value of h where the first Floquet exponent λ crosses the imaginary axis. For small damping constant g there will be sharp relative minima of $h_{\rm nc}(k)$ corresponding to modes fulfilling the parametric resonance condition $\omega_{\mathbf{k}} = \omega/2$. The absolute minimum (i.e., the lowest relative minimum) defines the actual threshold h_c and the critical wave number k_c.

We are looking for modes with a low number of nodes in the z direction. For thick films (i.e., $d \gg \sqrt{D}/\sqrt{4\pi}$) we can qualitatively distinguish between exchange modes and dipolar (i.e., magnetostatic) modes depending on whether the exchange terms or the dipolar terms in (7) dominate. For certain values of ω and k_c crossings between exchange modes and dipolar modes occur and a kind of "hybridization" will take place [9], which leads to an increase of the threshold. This makes it possible for a nonhybridized mode to become the most unstable mode [10]. Thus for certain values of ω (or H) there will occur a competition between modes with different in-plane wave numbers k_c but the same threshold. We will not further consider this interesting competition which may also lead to quasiperiodic patterns.

In this Letter we consider the case

$$k_c d \ll 0, \tag{8}$$

where it is possible to calculate the coefficients c and a of (4) analytically. Neglecting the hybridization with exchange modes we assume that the most unstable mode is the nodeless dipolar mode. Furthermore we make the approximation that this mode is uniform in z because of (8). Using this approximation ϕ can be eliminated in (7) in leading order of $k_c d$ by $\phi = -(m_+ + m_-)k_c d/4$. The uniformity in z drastically simplifies the calculation of the coefficients of the amplitude equation (4) mainly because in (5) no second-order terms of A_j occur. The coefficients are lengthy expressions containing time averages of products of $m_\pm$. The functional form of a is

$$a(\alpha) = \tfrac{4}{3} - \eta + (\tfrac{2}{3} + \eta)\cos 2\alpha - a_S \sin 2\alpha. \tag{9}$$

In order to get (9) it is not necessary to solve (7); only the uniformity assumption in z is required. In the case of weak damping (i.e., $g \ll 1$), a solution of (7) is very well approximated by the ansatz $m_-^* = m_+ = \mu_+\exp(i\omega t/2) + \mu_-\exp(-i\omega t/2)$, where $\mu_\pm$ are given by $\mu_+ = (1+\sqrt{1+\delta^2})(i-1)+O(g)$ and $\mu_- = \delta(i+1)+O(g)$, respectively, with $\delta = 2\pi\gamma M_0 k_c d/\omega$. In leading order of g and $k_c d$ the coefficients of (4) and (9) are

$$\tau_0 = \frac{2}{\omega g}, \quad c = \frac{48}{k_c d}, \quad \eta = \frac{16\pi}{9D}k_c^2, \quad a_S = \frac{4\pi\gamma M_0 k_c d}{3\omega g}. \tag{10}$$

Since $c > 0$, the bifurcation at the threshold is supercritical. Only in this case are the amplitude equations (4) useful to describe patterns and their dynamics. Note that $a_S \propto O(g^{-1})$. Thus the coupling a is dominated by the term which breaks the reflection symmetry. On the other hand, η is very small. It is determined by the part of the equation of motion which comes from the exchange interaction only. Below we will see that hexagonal patterns become unstable if η changes its sign and becomes negative. This sign change may be possible due to higher-order corrections in $k_c d$.

In order to investigate patterns described by the amplitude equation (4) it is convenient to introduce the ansatz $A_j(t) = [(\epsilon/c)P_j(2\epsilon t/\tau_0)]^{1/2}\exp[i\Psi_j(2\epsilon t/\tau_0)]$ which leads to

$$\dot{P}_j = \Big[1 - P_j - \sum_{l\neq j} a(\alpha_l - \alpha_j)P_l\Big]P_j, \quad \dot{\Psi}_j = 0. \tag{11}$$

The phase of each standing wave is constant, and is undetermined by the amplitude equation. Two of these phases are related to the translational invariance of an infinitely extended, uniform film. The other phases are related to so-called phason modes [11]. The dynamics of these modes is governed by higher-order terms of the amplitude equation.

Stationary patterns are N-wave patterns where N amplitudes of (11) are nonzero and all others are zero. For a given set of angles α_j such an N-wave pattern is uniquely determined by N linear algebraic equations. Since $P_j \geq 0$, not all values of the α_j's are allowed. In order to study the stability of these patterns we distinguish between internal and external stability. A pattern is internally stable if small disturbances of the amplitudes of the waves building the pattern decay exponentially, and externally stable if no additional waves grow up.

The simplest pattern is a one-wave pattern with amplitude $P = 1$. This pattern is externally unstable against waves with relative angles α between $-\pi/2-\alpha_1$ and $-\alpha_2$, where $0 < \alpha_{1/2} \propto g$. The fastest growing wave has an angle near $-45°$. This instability is caused by the dominant reflection-symmetry-breaking sine part. This is similar to the Küppers-Lortz instability of a rotating Rayleigh-Bénard system [12], which has rotational symmetry but where the rigid rotation breaks the reflection symmetry.

Contrary to the ferromagnetic case the symmetry is only weakly broken which means that the roll pattern becomes unstable only if the angular velocity is larger than some threshold.

Two-wave patterns exist only for angles from small intervals around 0° and 90°, with widths proportional to g. The patterns are stable only for angles from a subinterval located at 90°. Since $g \ll 1$, the square pattern is, roughly speaking, the only stable two-wave pattern.

Three-wave patterns exist only if the angles between any two wave vectors are less than 90° (see Fig. 1). The exact existence area in parameter space spanned by these angles is of order g smaller. For $0 < \eta < 5/6$, the—generally quasiperiodic—three-wave patterns are stable in a large area; only in small areas near the existence boundary does an external instability occur. In the limit $g \to 0$ the stability boundary does not depend on η. For negative η, around the point corresponding to the hexagonal pattern an area opens with internally and externally unstable patterns. The internal instability of the hexagonal pattern is caused by an oscillatory instability which leads to a supercritical Hopf bifurcation similar to a rotating Rayleigh-Bénard system with an angular velocity larger than the Küppers-Lortz threshold; the hexagonal pattern is unstable due to Hopf bifurcation, which leads to some kind of weak turbulence [13]. The Hopf frequency is $a_S/2$ in units $\tau_0/(2\epsilon)$ or $(2/3)\pi\gamma M_0 k_c d\,\epsilon$ in physical units; it is independent of g and should be much less than ω in order to be consistent with the assumption that the A_j vary on a longer time scale than the driving field. An interesting and open question is: Which pattern will the system select? The usual argument that the system selects the ground state does not work since the amplitude equation (4) cannot be derived from a Lyapunov function L (i.e., there exists no L such that $dA_j/dt = -\partial L/\partial A_j$) which could serve

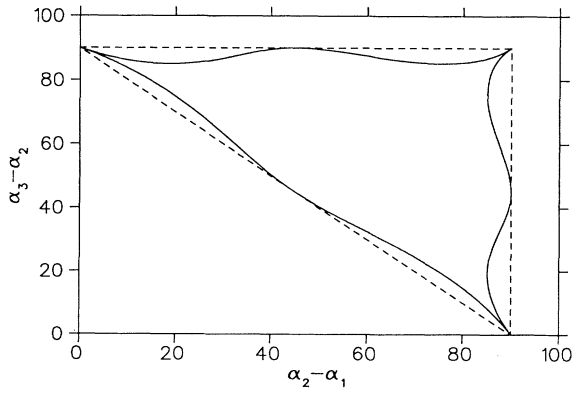

FIG. 1. Existence and stability boundary of three-wave solutions for $g \to 0$ (i.e., $a_s \to \infty$) and $0 < \eta < 5/6$. Dashed lines code the existence boundary and the internal stability boundary; they are nearly identical. Solid lines code the external stability boundary.

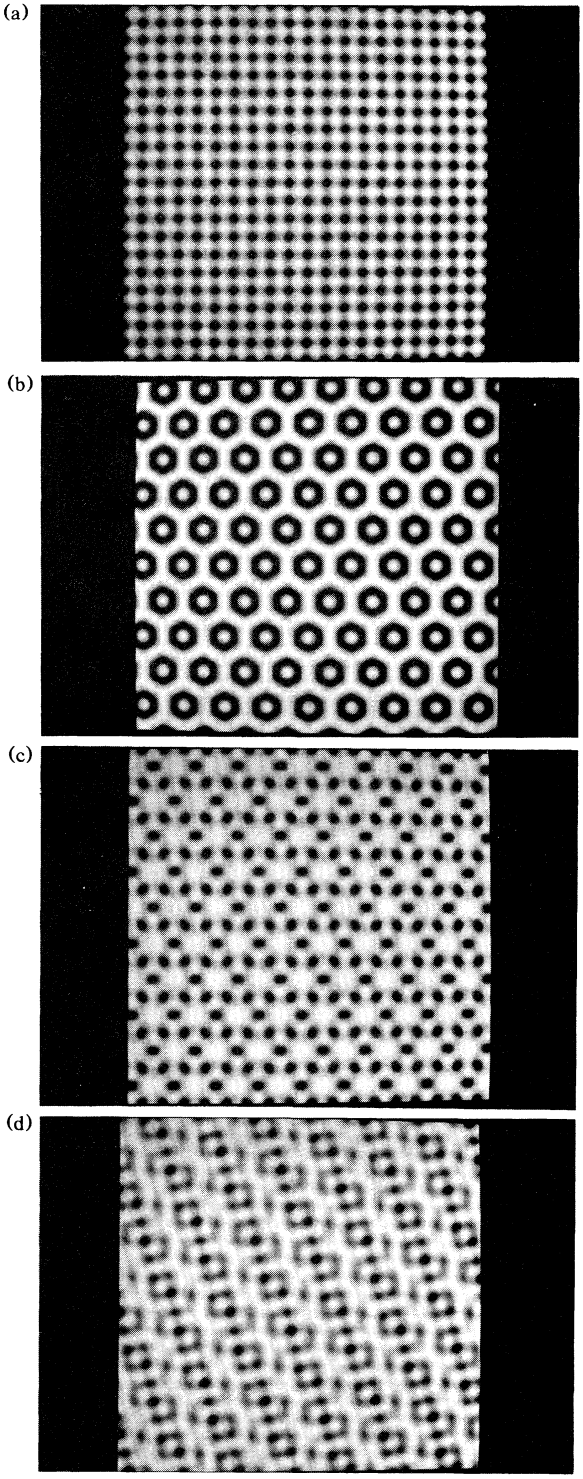

FIG. 2. Computer-generated images of several patterns: (a) Square; (b),(c) hexagonal patterns for different values of the phases Ψ_j; and (d) quasiperiodic pattern for $\alpha_2 - \alpha_1 = 80.21°$, $\alpha_3 - \alpha_2 = 57.30°$. The grey scale codes the time average of $M_x^2 + M_y^2$ where black means zero and white means maximum values. The side length of each image is $20\pi/k_c$.

as a potential energy.

All N-wave patterns with $N > 3$ seem to be unstable. For equidistant angles they are internally unstable. For arbitrary angles it is only a conjecture which is supported by numerical simulations of (4) using 48 waves with equidistant angles. Only squares and three-wave patterns survived in such simulations after starting with a random initial condition with small amplitudes.

In order to find out whether these patterns are observable in real experiments, we calculate the expected contrast of an experiment using Faraday rotation which measures the time average of M_z. The pattern contrast C_p is defined as the difference of the maximum and the minimum normalized by M_0,

$$C_p \equiv \left(\max_{x,y}\langle M_z\rangle - \min_{x,y}\langle M_z\rangle\right)\Big/ M_0, \tag{12}$$

where $\langle\ \rangle$ denotes the time average. For regular N-wave patterns (i.e., equidistant angles) we get in leading order in g and $k_c d$

$$C_p = \frac{k_c d}{[N(4-3\eta)-3]\sin^2 \pi/(2N)}\,\epsilon, \tag{13}$$

independent of g, which is a surprising result in view of the fact that the absorbed power is proportional to g. For squares and hexagons the contrast is $C_p^{(\mathrm{square})} = \frac{2}{5} k_c d\,\epsilon$ and $C_p^{(\mathrm{hexagon})} = \frac{4}{9} k_c d\,\epsilon$, respectively. Thus for $k_c d = 0.1$ and pumping power 2 dB above threshold (i.e., $\epsilon = 0.26$) one should get a contrast of ≈ 0.01 for hexagons which should be detectable by means of Faraday rotation [14]. Figure 2 shows computer-generated images for several patterns, simulating the expected images from experiments using Faraday rotation as an imaging technique. Note that the lattice constant of the visual square pattern is half that of the true pattern. The different hexagonal patterns are due to different values of Ψ_j.

In this Letter we have shown that squares and three-wave patterns (hexagons and quasiperiodic patterns) are stable dissipative patterns in an out-of-plane parallel-pumped ferromagnetic insulating film. This result was derived in the limit pumping power near critical pumping power ($\epsilon \to 0$), critical wavelength much greater than film thickness ($k_c d \to 0$), and weak damping ($g \to 0$). What can one expect if one is not in this limit? The amplitude equation will be true as long as $\epsilon \ll 1$ independent of the values of $k_c d$ and g. Only the coefficients, especially the nonlinear ones (i.e., a and c), may change, with the consequence that, e.g., hexagons may become oscillatory unstable. It is not possible to say for which values of ϵ the amplitude equation is no longer a good description of the dynamics. This may be determined by performing suitable experiments.

I gratefully acknowledge helpful discussions with S. Schultz, H. Suhl, and H. Thomas. This work was started during my stay at the University of California at San Diego and I thank H. Suhl for his hospitality. I also thank R. Hofer and H.-J. Hug for preparing the images. This work was supported by the Volkswagenstiftung and the Swiss National Science Foundation.

[1] See, e.g., *Hydrodynamic Instabilities and The Transition to Turbulence*, edited by H. L. Swinney and J. P. Gollub, Topics in Applied Physics Vol. 45 (Springer, Berlin, 1981); P. Manneville, *Dissipative Structures and Weak Turbulence* (Academics, Boston, 1990).

[2] See, e.g., S. T. Milner, J. Fluid Mech. **225**, 81 (1991), and references therein.

[3] N. Bloembergen and R. W. Damon, Phys. Rev. **85**, 699 (1952); R. W. Damon, Rev. Mod. Phys. **25**, 239 (1953); N. Bloembergen and S. Wang, Phys. Rev. **93**, 72 (1954).

[4] H. Suhl, Phys. Rev. **101**, 1437 (1956); J. Phys. Chem. Solids **1**, 209 (1957).

[5] See, e.g., E. V. Astashkina and A. S. Mikhailov, Zh. Eksp. Teor. Fiz. **78**, 1636 (1980) [Sov. Phys. JETP **51**, 821 (1980)]; V. L. Grankin, V. S. L'vov, V. I. Motorin, and S. L. Musher, Zh. Eksp. Teor. Fiz. **81**, 757 (1981) [Sov. Phys. JETP **54**, 405 (1981)]; K. Nakamura, S. Ohta, and K. Kawasaki, J. Phys. C **15**, L143 (1982); G. Gibson and C. Jeffries, Phys. Rev. A **29**, 811 (1984); F. Waldner, Phys. Rev. A **31**, 420 (1985); X. Y. Zhang and H. Suhl, Phys. Rev. A **32**, 2530 (1985); S. M. Rezende, F. M. de Aguiar, and O. F. de Alcantara Bonfim, J. Magn. Magn. Mater. **54-57**, 1127 (1986); T. L. Carroll, L. M. Pecora, and F. J. Rachford, Phys. Rev. Lett. **59**, 2891 (1987); P. H. Bryant, C. D. Jeffries, and K. Nakamura, Phys. Rev. A **38**, 4223 (1988); G. Wiese and H. Benner, Z. Phys. B **79**, 119 (1990).

[6] Y. A. Gaidai, I. I. Kondilenko, and A. A. Solomko, Pis'ma Zh. Eksp. Teor. Fiz. **21**, 575 (1975) [JETP Lett. **21**, 269 (1975)]; W. Wettling, W. D. Wilber, P. Kabos, and C. E. Patton, Phys. Rev. Lett. **51**, 1680 (1983).

[7] We are not concerned with magnetostatic modes excited by nonuniform pumping where nice images of these modes exist; see, e.g., J. F. Dillon, Jr., H. Kamimura, and J. P. Remeika, J. Appl. Phys. **34**, 1240 (1963).

[8] See, e.g., R. W. Damon, in *Magnetism*, edited by G. T. Rado and H. Suhl (Academic, New York, 1963), Vol. 1.

[9] Y. V. Gribkova and M. I. Kaganov, Fiz. Tverd. Tela **33**, 508 (1991) [Sov. Phys. Solid State **33**, 290 (1991)].

[10] F. J. Elmer (unpublished).

[11] B. A. Malomed, A. A. Nepomnyashchii, and M. I. Tribelskii, Zh. Eksp. Teor. Fiz. **96**, 684 (1989) [Sov. Phys. JETP **69**, 388 (1989)].

[12] G. Küppers and D. Lortz, J. Fluid Mech. **35**, 609 (1969).

[13] F. H. Busse and K. E. Heikes, Science **208**, 173 (1980); Y. Tu and M. C. Cross, Phys. Rev. Lett. **69**, 2515 (1992).

[14] S. Schultz (private communication).

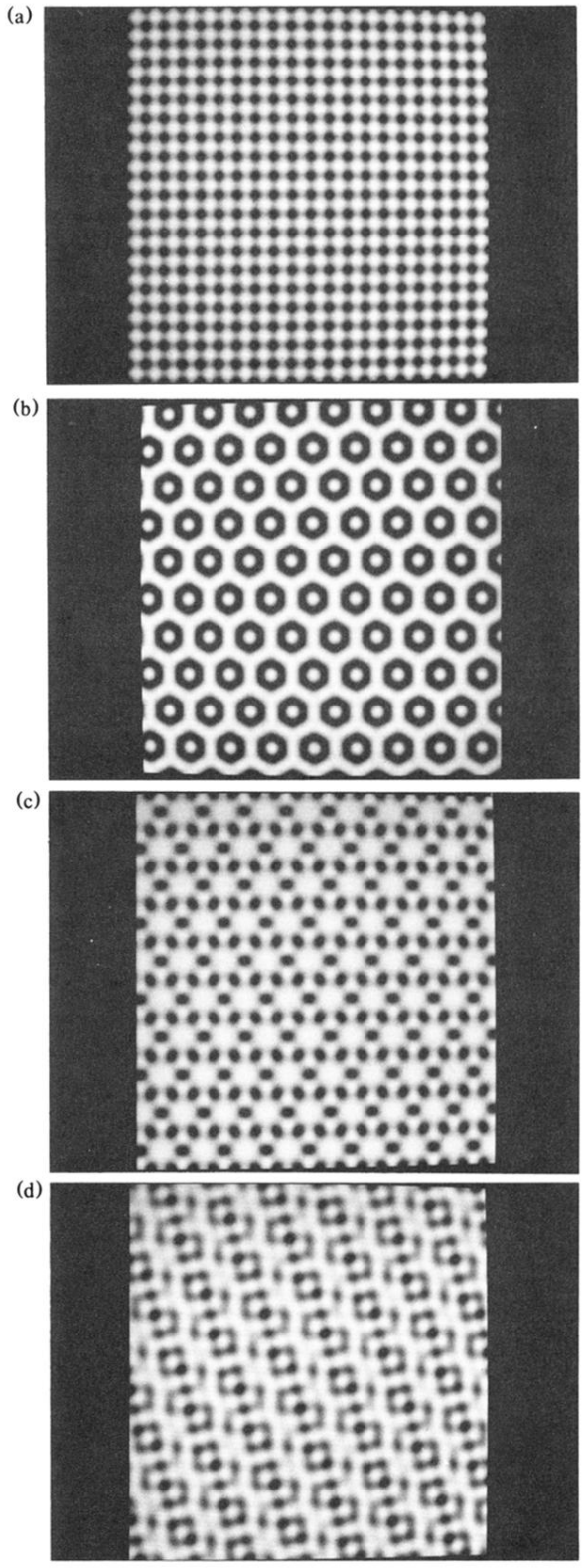

FIG. 2. Computer-generated images of several patterns: (a) Square; (b),(c) hexagonal patterns for different values of the phases Ψ_j; and (d) quasiperiodic pattern for $\alpha_2 - \alpha_1 = 80.21°$, $\alpha_3 - \alpha_2 = 57.30°$. The grey scale codes the time average of $M_x^2 + M_y^2$ where black means zero and white means maximum values. The side length of each image is $20\pi/k_c$.